

## Supporting Information

---

### **Singlet Oxygen Photophysics in Liquid Solvents: Converging on a Unified Picture**

Mikkel Bregnhøj,<sup>a</sup> Michael Westberg,<sup>a</sup> Boris F. Minaev,<sup>b</sup> and Peter R. Ogilby<sup>a\*</sup>

<sup>a</sup> Department of Chemistry, Aarhus University, DK-8000, Aarhus, Denmark

<sup>b</sup> Department of Natural Sciences, Bogdan Khmel'nitsky National University, Cherkassy, Ukraine

## Contents

Examples of $O_2(a^1\Delta_g)$ kinetic data .....	S3
Compiled $O_2(a^1\Delta_g)$ and $O_2(b^1\Sigma_g^+)$ Data.....	S5
Static dielectric constant .....	S11
Spectral bandwidth.....	S12
More detailed theoretical considerations on the radiative transitions.....	S13
Solvatochromic effects.....	S19
References .....	S20

## Examples of O<sub>2</sub>(a<sup>1</sup>Δ<sub>g</sub>) kinetic data

### Photosensitized experiments

The most common way to produce O<sub>2</sub>(a<sup>1</sup>Δ<sub>g</sub>) is by energy transfer from the lowest excited triplet state of a photosensitizer, <sup>3</sup>Sens<sub>1</sub>, to ground state oxygen, O<sub>2</sub>(X<sup>3</sup>Σ<sub>g</sub><sup>-</sup>). In a time-resolved a → X phosphorescence experiment, one can simultaneously obtain information about the kinetics of O<sub>2</sub>(a<sup>1</sup>Δ<sub>g</sub>) formation and decay as well as the amount of O<sub>2</sub>(a<sup>1</sup>Δ<sub>g</sub>) produced.

In a typical homogenous solution, the a → X phosphorescence signal can be modelled using eq S1.<sup>1, 2</sup>

$$[\text{O}_2(\text{a}^1\Delta_{\text{g}})](t) = \frac{k_{\text{form}}[\text{O}_2(\text{X}^3\Sigma_{\text{g}}^-)][^3\text{Sens}_1]_0}{\tau_{\Delta}^{-1} - \tau_{\text{T}}^{-1}} \left( \exp\left(-\frac{t}{\tau_{\text{T}}}\right) - \exp\left(-\frac{t}{\tau_{\Delta}}\right) \right) \quad (\text{S1})$$

In this equation, [O<sub>2</sub>(X<sup>3</sup>Σ<sub>g</sub><sup>-</sup>)] and [<sup>3</sup>Sens<sub>1</sub>]<sub>0</sub> are the concentrations of ground state oxygen and the sensitizer triplet state at t = 0, respectively, k<sub>form</sub> is the rate constant for O<sub>2</sub>(a<sup>1</sup>Δ<sub>g</sub>) formation, τ<sub>Δ</sub> the lifetime of O<sub>2</sub>(a<sup>1</sup>Δ<sub>g</sub>), and τ<sub>T</sub> the lifetime of the sensitizer triplet state. An example of typical data obtained in D<sub>2</sub>O is given in Figure S1.

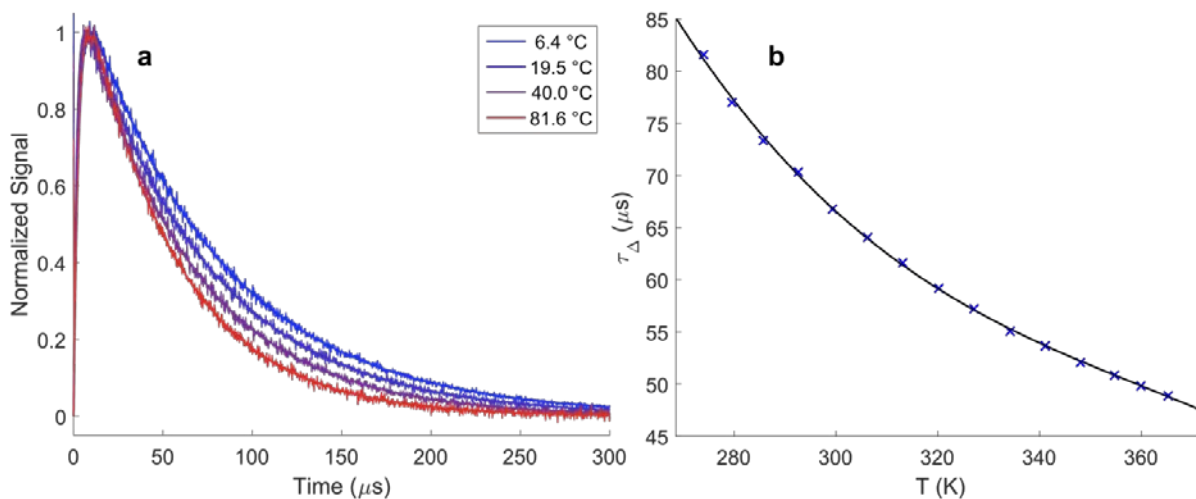


**Fig. S1** Time-resolved O<sub>2</sub>(a<sup>1</sup>Δ<sub>g</sub>) phosphorescence signals recorded upon 420 nm pulsed laser irradiation of the sensitizer 1H-phenalen-1-one-2-sulfonic acid, PNS, in buffered D<sub>2</sub>O as a function of temperature. A fit to eq S1 is superimposed on each kinetic trace. The concentration of PNS is ~ 5 μM. For each trace, data were acquired over 1 min using a laser power of ~ 200 μW at a repetition rate of 1 kHz. This figure is made from published data.<sup>3</sup>

## Direct excitation experiments

In systems and experiments where the use of sensitizers is undesirable, a good approach to produce  $O_2(a^1\Delta_g)$  is direct excitation of the  $X \rightarrow b$  transition at 765 nm.<sup>3-7</sup> This technique selectively produces  $O_2(b^1\Sigma_g^+)$ , which subsequently decays rapidly with near unity yield to  $O_2(a^1\Delta_g)$ . Although the solvent-dependent absorption coefficients for this transition in oxygen are small (*vide infra*), a sufficient amount of  $O_2(a^1\Delta_g)$  can nevertheless be produced for a wide range of experiments.<sup>3-7</sup>

In these experiments,  $a \rightarrow X$  phosphorescence can likewise be detected upon 765 nm pulsed laser irradiation of a neat solvent. Moreover, the immediate precursor to  $O_2(a^1\Delta_g)$  is  $O_2(b^1\Sigma_g^+)$ , which is very short-lived ( $< 1$  ns). Therefore, we can discern no rise in our  $O_2(a^1\Delta_g)$  phosphorescence signals, and the lifetime of  $O_2(a^1\Delta_g)$  can be extracted using a simple mono-exponential decay function. An example of typical direct excitation data is given in Figure S2.

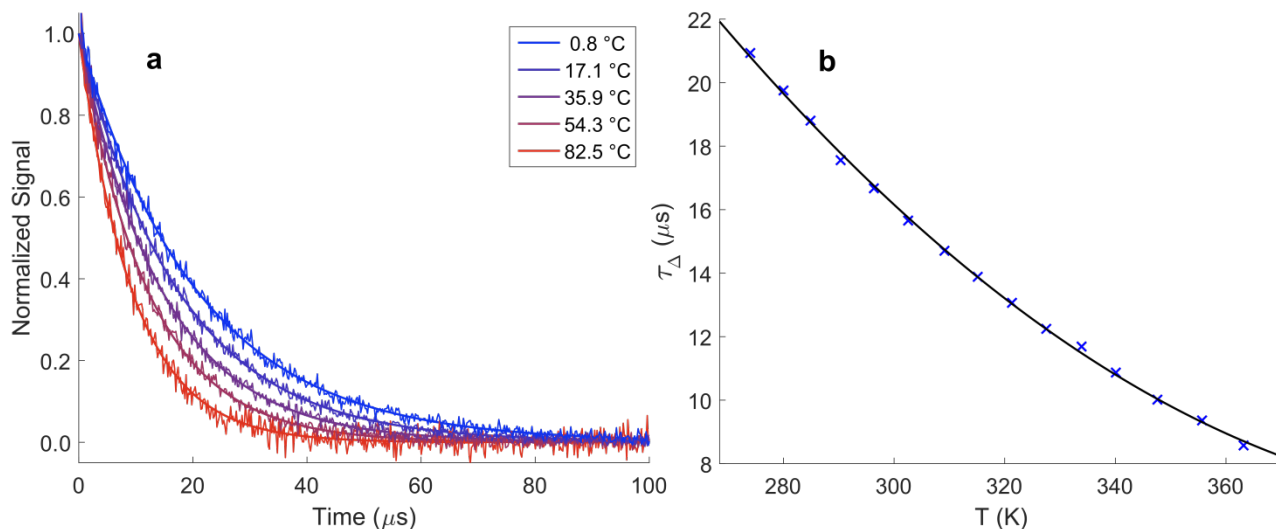


**Fig. S2** Time-resolved  $O_2(a^1\Delta_g)$  phosphorescence signals recorded upon 765 nm pulsed laser irradiation of neat oxygenated mesitylene as a function of temperature. A mono-exponential fit is superimposed on each kinetic trace. For each trace, data were acquired over 3 min using an incident laser power of  $\sim 200$  mW at a repetition rate of 1 kHz. This figure is adapted from published material.<sup>3</sup>

## Compiled $O_2(a^1\Delta_g)$ and $O_2(b^1\Sigma_g^+)$ Data

The data shown below have been critically compiled from sources exclusively devoted to the study of singlet oxygen photophysics in liquids. These tables represent, what we believe, is the most accurate set of data known to date.

**Table S1:** The lifetime of  $O_2(a^1\Delta_g)$  and  $O_2(b^1\Sigma_g^+)$  in air-saturated solutions at room temperature.

Solvent	$\tau_\Delta$ ( $\mu$ s)	$\tau_\Sigma$ (ps)
Water	$3.5 \pm 0.1^a$	$8.2 \pm 0.8^h$
Water- $d_2$ ( $D_2O$ )	$68.9 \pm 1.4^a$	$42 \pm 4.2^h$
Methanol	$9.9 \pm 0.3^c$	$18 \pm 1.8^h$
Methanol- $d$ ( $CH_3OD$ )	$31.4 \pm 0.6^a$	-
Methanol- $d_4$	$276 \pm 6^a$	$94 \pm 9.4^h$
Ethanol	$15.3 \pm 0.8^d$	-
Ethanol- $d$ ( $CH_3CH_2OD$ )	$30.5 \pm 0.5^d$	-
Ethanol- $d_6$	$23^d$	-
1-propanol	$15.9 \pm 0.3^a$	-
2-propanol	$22.1 \pm 1.1^d$	-
2-methyl-2-propanol	$30.8 \pm 1.5^d$	-
2-methyl-1-propanol	$21.1 \pm 1.1^d$	-
1-butanol	$17.5 \pm 0.9^d$	-
2-butanol	$19.7 \pm 1.0^d$	-
1-pentanol	$17.8 \pm 0.9^d$	-
1-hexanol	$17.9 \pm 0.9^d$	-
Cyclohexanol	$15.1 \pm 0.8^d$	-
1-heptanol	$18.1 \pm 0.9^d$	-
1-octanol	$18.5 \pm 0.3^c$	-
1-nonanol	$18.6 \pm 0.9^d$	-
1-decanol	$17.8 \pm 0.9^d$	-
2,2,2-trifluoroethanol	$30.5 \pm 1.0^c$	-
Acetone	$45.6 \pm 0.9^a$	$123 \pm 12^h$
Acetone- $d_6$	$1039 \pm 21^a$	$294 \pm 29^h$
Acetonitrile	$81 \pm 1.6^a$	$134 \pm 13^h$
Acetonitrile- $d_3$	$1610 \pm 32^a$	$613 \pm 61^h$
Benzonitrile	$40.0 \pm 0.8^a$	-
Benzene	$30.4 \pm 0.6^a$	$135 \pm 14^h$
Benzene- $d_6$	$747 \pm 15^a$	$279 \pm 28^h$
Toluene	$30.5 \pm 0.6^a$	-
Toluene- $d_8$	$314 \pm 6^a$	-
<i>o</i> -xylene	$23.4 \pm 0.5^a$	-
<i>o</i> -xylene- $d_{10}$	$87 \pm 2^b$	-
Mesitylene	$16.9 \pm 0.3^a$	-
Mesitylene- $d_{12}$	$31.8 \pm 0.6^b$	-
Ethylbenzene	$26^d$	-
Butylbenzene	$25^d$	-
Benzyl alcohol	$14.4 \pm 0.3^a$	-
Trifluorotoluene	$61.7 \pm 1.2^a$	-
Fluorobenzene	$45.8 \pm 2.5^d$	-
Chlorobenzene	$43.6 \pm 0.9^a$	-

<b>Bromobenzene</b>	42.5 ± 0.2 <sup>c</sup>	-
<b>Bromobenzene-<i>d</i><sub>5</sub></b>	1360 ± 20 <sup>e</sup>	-
<b>Iodobenzene</b>	38.9 ± 0.8 <sup>a</sup>	-
<b><i>o</i>-dichlorobenzene</b>	57.0 ± 1.1 <sup>a</sup>	-
<b>1,2,4-trichlorobenzene</b>	93.8 ± 1.9 <sup>a</sup>	-
<b>Hexafluorobenzene</b>	30000 ± 3000 <sup>f</sup>	12600 ± 1260 <sup>h</sup>
<b>Chloropentafluorobenzene</b>	24500 ± 2000 <sup>e</sup>	-
<b>Bromopentafluorobenzene</b>	21900 ± 1000 <sup>e</sup>	-
<b>Iodopentafluorobenzene</b>	15100 ± 1000 <sup>e</sup>	-
<b>Tetrahydrofuran (THF)</b>	23.5 ± 4 <sup>d</sup>	-
<b>1,4-dioxane</b>	26.7 ± 1.3 <sup>d</sup>	-
<b>Cyclohexane</b>	24.0 ± 0.5 <sup>a</sup>	83 ± 8.3 <sup>h</sup>
<b>Cyclohexane-<i>d</i><sub>12</sub></b>	483 ± 10 <sup>a</sup>	-
<b><i>n</i>-pentane</b>	34.8 ± 0.7 <sup>a</sup>	-
<b>2,2,4-trimethylpentane (isooctane)</b>	37.6 ± 1.9 <sup>d</sup>	-
<b><i>n</i>-hexane</b>	32.2 ± 0.6 <sup>a</sup>	-
<b><i>n</i>-hexane-<i>d</i><sub>14</sub></b>	586 ± 12 <sup>a</sup>	-
<b><i>n</i>-heptane</b>	30.1 ± 0.6 <sup>a</sup>	-
<b><i>n</i>-octane</b>	28.6 ± 0.6 <sup>a</sup>	-
<b><i>n</i>-nonane</b>	23.7 ± 1.2 <sup>d</sup>	-
<b><i>n</i>-decane</b>	26.5 ± 0.5 <sup>a</sup>	-
<b>Carbon tetrachloride</b>	128000 ± 12800 <sup>f</sup>	150000 ± 15000 <sup>h</sup>
<b>Chloroform</b>	229 ± 12 <sup>f</sup>	1180 ± 118 <sup>h</sup>
<b>Chloroform-<i>d</i></b>	9400 ± 500 <sup>g</sup>	2220 ± 222 <sup>h</sup>
<b>Dichloromethane</b>	95.7 ± 1 <sup>c</sup>	-
<b>Dichloromethane-<i>d</i><sub>2</sub></b>	120 <sup>d</sup>	-
<b>1,2-dichloroethane</b>	63.2 ± 3.16 <sup>d</sup>	-
<b>Tetrachloroethylene</b>	1250 ± 50 <sup>d</sup>	200000 ± 20000 <sup>h</sup>
<b>Diiodomethane</b>	55.5 ± 0.4 <sup>c</sup>	-
<b>Perchlorobutadiene</b>	-	90000 ± 9000 <sup>h</sup>
<b>Perfluorohexane</b>	214000 ± 21400 <sup>f</sup>	-
<b>1-iodoperfluorohexane</b>	53000 ± 5300 <sup>f</sup>	-
<b>1,2-dibromotetrafluoroethane</b>	111000 ± 11100 <sup>f</sup>	-
<b>1,1,2-trichloro-1,1,2-trifluoroethane (Freon 113)</b>	133000 ± 13300 <sup>f</sup>	47700 ± 4770 <sup>h</sup>
<b>Trichlorofluoromethane (Freon 11)</b>	24000 ± 1000 <sup>g</sup>	-
<b>Diethyl ether</b>	30.4 ± 1.5 <sup>d</sup>	-
<b>Ethyl acetate</b>	45 <sup>d</sup>	-
<b>Carbon disulfide</b>	79000 ± 7900 <sup>f</sup>	30000 ± 3000 <sup>h</sup>
<b>Perfluorodecalin</b>	309000 ± 30900 <sup>f</sup>	-
<b>N,N-dimethylformamide (DMF)</b>	19.3 ± 4.5 <sup>d</sup>	-

<sup>a</sup> From Bregnhøj, *et al.*<sup>3</sup>

<sup>b</sup> Unpublished data.

<sup>c</sup> From Bregnhøj, *et al.*<sup>6</sup>

<sup>d</sup> From the database of Wilkinson, *et al.*<sup>8</sup> The given value is the average of selected entries in this compilation with the standard deviation given as the error.

<sup>e</sup> From Schmidt.<sup>9</sup>

<sup>f</sup> From Schmidt and Afshari.<sup>10</sup>

<sup>g</sup> From Schmidt and Brauer.<sup>11</sup>

<sup>h</sup> From Weldon, *et al.*<sup>12</sup> and references therein.

**Table S2:** Spectral data for the  $O_2(a^1\Delta_g) \rightarrow O_2(X^3\Sigma_g^-)$  transition.

Solvent	$\nu_{\max}^{aX}$ (cm <sup>-1</sup> )	$\Delta\nu_{FWHM}^{aX}$ (cm <sup>-1</sup> )	$k_T^{aX}$ (s <sup>-1</sup> )
Gas-phase	7882.4 ± 1 <sup>b</sup>	-	2.3 × 10 <sup>-4</sup> <sup>h</sup>
Water	7849.1 ± 3 <sup>a</sup>	108.4 ± 6 <sup>a</sup>	0.16 ± 0.016 <sup>e,f</sup>
Water- <i>d</i> <sub>2</sub> (D <sub>2</sub> O)	7849.7 ± 1 <sup>a</sup>	108.3 ± 2 <sup>a</sup>	0.19 ± 0.019 <sup>e,f</sup>
Methanol	7853.2 ± 1 <sup>a</sup>	125.4 ± 2 <sup>a</sup>	0.35 ± 0.035 <sup>e,f</sup>
Methanol- <i>d</i> <sub>4</sub>	7851.4 ± 1 <sup>a,b</sup>	122.9 ± 4 <sup>a,b</sup>	-
Ethanol	7856.8 ± 3 <sup>a</sup>	119.8 ± 6 <sup>a</sup>	0.55 ± 0.055 <sup>g</sup>
Ethanol- <i>d</i> (CH <sub>3</sub> CH <sub>2</sub> OD)	-	-	0.35 ± 0.035 <sup>e</sup>
Ethanol- <i>d</i> <sub>6</sub>	7856.5 ± 1 <sup>a</sup>	120.3 ± 2 <sup>a</sup>	-
1-propanol	7855.6 ± 1 <sup>a</sup>	111.7 ± 2 <sup>a</sup>	0.47 ± 0.047 <sup>e</sup>
2-propanol	-	-	0.47 ± 0.047 <sup>e</sup>
1-butanol	7853.8 ± 1 <sup>a</sup>	104.5 ± 2 <sup>a</sup>	0.44 ± 0.044 <sup>e</sup>
2-butanol	-	-	0.57 ± 0.057 <sup>e</sup>
1-pentanol	7852.3 ± 1 <sup>a</sup>	102.2 ± 2 <sup>a</sup>	-
1-hexanol	7851.7 ± 1 <sup>a</sup>	98.5 ± 2 <sup>a</sup>	-
1-octanol	7851.2 ± 1 <sup>a</sup>	96.8 ± 2 <sup>a</sup>	-
1-nonanol	7850.4 ± 1 <sup>a</sup>	95 ± 2 <sup>a</sup>	-
1-decanol	7850.2 ± 1 <sup>a</sup>	95.1 ± 2 <sup>a</sup>	-
2,2,2-trifluoroethanol	7869.2 ± 1 <sup>a</sup>	84.5 ± 2 <sup>a</sup>	0.25 ± 0.025 <sup>e,f</sup>
Acetone	7852.6 ± 1 <sup>a</sup>	121.1 ± 2 <sup>a</sup>	0.56 ± 0.056 <sup>e,f</sup>
Acetone- <i>d</i> <sub>6</sub>	7849.0 ± 1 <sup>b</sup>	114 ± 5 <sup>b</sup>	-
Acetonitrile	7851.5 ± 1 <sup>a</sup>	125.3 ± 2 <sup>a</sup>	0.45 ± 0.045 <sup>e</sup>
Acetonitrile- <i>d</i> <sub>3</sub>	7849.9 ± 1 <sup>a,b</sup>	122.2 ± 4 <sup>a,b</sup>	-
Benzonitrile	7836.3 ± 1 <sup>a</sup>	106.3 ± 2 <sup>a</sup>	1.80 ± 0.18 <sup>e</sup>
1,1,1-trifluoro acetic acid	7873.2 ± 3 <sup>a</sup>	86.9 ± 6 <sup>a</sup>	-
1,1,1-trifluoro acetic acid- <i>d</i>	7870.8 ± 3 <sup>b</sup>	90 ± 15 <sup>b</sup>	-
Formic acid	-	-	0.25 ± 0.025 <sup>g</sup>
Propionic acid	-	-	0.79 ± 0.079 <sup>g</sup>
Benzene	7839.5 ± 1 <sup>a</sup>	115.9 ± 2 <sup>a</sup>	1.50 ± 0.5 <sup>e,f,g,i</sup>
Benzene- <i>d</i> <sub>6</sub>	7838.8 ± 2 <sup>a,b</sup>	115.9 ± 1 <sup>a,b</sup>	1.34 ± 0.13 <sup>f</sup>
Toluene	7839.7 ± 1 <sup>a,c</sup>	112.9 ± 2 <sup>a,c</sup>	1.44 ± 0.14 <sup>e</sup>
Toluene- <i>d</i> <sub>8</sub>	7838.8 ± 1 <sup>b</sup>	114.5 ± 5 <sup>b</sup>	1.47 ± 0.15 <sup>g</sup>
<i>p</i> -xylene	7840.6 ± 1 <sup>a</sup>	109.6 ± 2 <sup>a</sup>	1.70 ± 0.17 <sup>g</sup>
Mesitylene	-	-	1.72 ± 0.17 <sup>g</sup>
1,2,4-trimethylbenzene	-	-	2.00 ± 0.20 <sup>g</sup>
Benzyl alcohol	7832.5 ± 1 <sup>a</sup>	115.5 ± 2 <sup>a</sup>	-
Trifluorotoluene	7856.2 ± 1 <sup>a</sup>	94.5 ± 2 <sup>a</sup>	1.14 ± 0.11 <sup>e</sup>
1,3-dibromobenzene	-	-	2.72 ± 0.27 <sup>e</sup>
Fluorobenzene	7844.4 ± 1 <sup>a</sup>	107.2 ± 2 <sup>a</sup>	1.28 ± 0.13 <sup>e</sup>
Chlorobenzene	7839.6 ± 1 <sup>a</sup>	109.6 ± 2 <sup>a</sup>	1.68 ± 0.17 <sup>e</sup>
Bromobenzene	7832.8 ± 1 <sup>a</sup>	112.4 ± 2 <sup>a</sup>	1.97 ± 0.20 <sup>e</sup>
Bromobenzene- <i>d</i> <sub>5</sub>	-	-	2.07 ± 0.21 <sup>f</sup>
Iodobenzene	7824.1 ± 1 <sup>a</sup>	123.7 ± 2 <sup>a</sup>	2.61 ± 0.26 <sup>e</sup>
Hexafluorobenzene	7867.4 ± 1 <sup>b</sup>	82.5 ± 5 <sup>b</sup>	0.51 ± 0.051 <sup>f</sup>
Chloropentafluorobenzene	7862.6 ± 1 <sup>b</sup>	95.0 ± 5 <sup>b</sup>	0.89 ± 0.089 <sup>f</sup>
Bromopentafluorobenzene	7859.1 ± 1 <sup>b</sup>	88.3 ± 5 <sup>b</sup>	1.25 ± 0.13 <sup>f</sup>
Iodopentafluorobenzene	7852.7 ± 1 <sup>b</sup>	96.3 ± 5 <sup>b</sup>	1.23 ± 0.12 <sup>f</sup>
Anisole	-	-	1.80 ± 0.18 <sup>g</sup>
<i>p</i> -chloroanisole	-	-	2.20 ± 0.22 <sup>g</sup>
<i>p</i> -bromoanisole	-	-	1.90 ± 0.19 <sup>g</sup>
1,3-dimethoxybenzene	-	-	1.90 ± 0.19 <sup>g</sup>

Tetrahydrofuran (THF)	7848.1 ± 1 <sup>a</sup>	118.5 ± 2 <sup>a</sup>	0.62 ± 0.062 <sup>e</sup>
1,4-dioxane	7841.6 ± 1 <sup>a</sup>	119.3 ± 2 <sup>a</sup>	0.56 ± 0.056 <sup>e</sup>
Pyridine	7834.7 ± 1 <sup>c</sup>	116.8 ± 2 <sup>c</sup>	-
Pyridine- <i>d</i> <sub>5</sub>	7831.6 ± 3 <sup>b</sup>	117 ± 15 <sup>b</sup>	-
1-methylnaphthalene	7825.5 ± 1 <sup>a</sup>	116.7 ± 2 <sup>a</sup>	2.96 ± 0.30 <sup>e</sup>
1-bromonaphthalene	7824.4 ± 1 <sup>a</sup>	112.0 ± 2 <sup>a</sup>	3.11 ± 0.31 <sup>e</sup>
2-ethylnaphthalene	-	-	2.03 ± 0.20 <sup>e</sup>
Cyclohexane	7853.8 ± 1 <sup>a</sup>	101.8 ± 2 <sup>a</sup>	0.66 ± 0.066 <sup>e</sup>
<i>n</i> -pentane	7859.8 ± 1 <sup>a</sup>	97.1 ± 2 <sup>a</sup>	0.47 ± 0.047 <sup>g</sup>
<i>n</i> -hexane	7858.2 ± 1 <sup>a</sup>	97.6 ± 2 <sup>a</sup>	0.60 ± 0.060 <sup>g</sup>
<i>n</i> -heptane	7856.8 ± 1 <sup>a</sup>	96.0 ± 2 <sup>a</sup>	0.66 ± 0.066 <sup>e</sup>
<i>n</i> -octane	7858.0 ± 1 <sup>a</sup>	94.1 ± 2 <sup>a</sup>	-
<i>n</i> -nonane	7855.0 ± 1 <sup>a</sup>	94.2 ± 2 <sup>a</sup>	-
<i>n</i> -decane	7854.2 ± 1 <sup>a</sup>	93.6 ± 2 <sup>a</sup>	-
1-hexene	7855.2 ± 1 <sup>a</sup>	102.4 ± 2 <sup>a</sup>	-
Carbon tetrachloride (CCl <sub>4</sub> )	7849.7 ± 1 <sup>a,b</sup>	102.8 ± 4 <sup>a,b</sup>	1.06 ± 0.11 <sup>e,f,g</sup>
Chloroform	7847.2 ± 2 <sup>a,b</sup>	106.8 ± 9 <sup>a,b</sup>	1.05 ± 0.11 <sup>e,f</sup>
Chloroform- <i>d</i>	7846.8 ± 1 <sup>b</sup>	107.3 ± 5 <sup>b</sup>	-
Dichloromethane	7837.0 ± 3 <sup>b</sup>	125 ± 15 <sup>b</sup>	0.75 ± 0.075 <sup>e</sup>
Dichloromethane- <i>d</i> <sub>2</sub>	7845.0 ± 1 <sup>b</sup>	113.8 ± 5 <sup>b</sup>	-
Dibromomethane	-	-	0.80 ± 0.080 <sup>g</sup>
1,2-dichloroethane	-	-	0.75 ± 0.075 <sup>g</sup>
Tetrachloroethylene	7847.0 ± 1 <sup>a,b</sup>	93.2 ± 4 <sup>a,b</sup>	1.89 ± 0.19 <sup>f</sup>
Diiodomethane	7800 <sup>d</sup>	-	4.08 ± 0.41 <sup>e</sup>
1-iodopropane	-	-	1.44 ± 0.14 <sup>e</sup>
Perchlorobutadiene	7844.2 ± 1 <sup>b</sup>	92.5 ± 5 <sup>b</sup>	1.85 ± 0.19 <sup>f</sup>
Dibromodifluoromethane	7857.7 ± 1 <sup>b</sup>	99.5 ± 5 <sup>b</sup>	-
Perfluorohexane	7881.5 ± 1 <sup>b</sup>	74.0 ± 5 <sup>b</sup>	-
1-iodoperfluorohexane	-	-	1.41 ± 0.14 <sup>f</sup>
1,2-dibromotetrafluoroethane	7863.5 ± 1 <sup>b</sup>	94.5 ± 5 <sup>b</sup>	1.40 ± 0.14 <sup>f</sup>
1,1,2-trichloro-1,2,2-trifluoroethane (Freon 113)	7865.4 ± 1 <sup>b</sup>	92.5 ± 5 <sup>b</sup>	1.35 ± 0.14 <sup>g</sup>
Trichlorofluoromethane (Freon 11)	7859.4 ± 1 <sup>b</sup>	99.5 ± 5 <sup>b</sup>	-
Diethyl ether	-	-	0.62 ± 0.062 <sup>g</sup>
Diphenyl ether	-	-	2.0 ± 0.20 <sup>g</sup>
2-nitropropane	-	-	0.19 ± 0.019 <sup>g</sup>
Acetic anhydride	-	-	0.53 ± 0.053 <sup>g</sup>
Diphenyl sulfide	-	-	2.66 ± 0.27 <sup>e</sup>
Carbon disulfide (CS <sub>2</sub> )	7828.3 ± 1 <sup>a,b</sup>	122.1 ± 4 <sup>a,b</sup>	3.13 ± 0.31 <sup>e,f</sup>
Perfluorodecalin	7882.2 ± 1 <sup>b</sup>	68.0 ± 5 <sup>b</sup>	-
Perfluoroperhydrophenanthrene	7881.8 ± 1 <sup>b</sup>	63.5 ± 5 <sup>b</sup>	-
N,N-dimethylformamide (DMF)	-	-	0.63 ± 0.063 <sup>g</sup>

<sup>a</sup> From Wessel and Rodgers.<sup>13</sup>

<sup>b</sup> From MacPherson and Truscott.<sup>14</sup>

<sup>c</sup> From Dam, *et al.*<sup>15</sup>

<sup>d</sup> From Ogilby.<sup>16</sup>

<sup>e</sup> From Poulsen, *et al.*<sup>17</sup> and references therein.

<sup>f</sup> From Hild and Schmidt<sup>18</sup> and references therein.

<sup>g</sup> From Darmanyán<sup>19</sup> and references therein.

<sup>h</sup> From Schweitzer and Schmidt.<sup>20</sup>

<sup>i</sup> From Schmidt.<sup>21</sup>

**Table S3:** Spectral data for the  $O_2(b^1\Sigma_g^+) \leftrightarrow O_2(a^1\Delta_g)$  transition.

Solvent	$\nu_{\max}^{ab}$ ( $\text{cm}^{-1}$ )	$\Delta\nu_{\text{FWHM}}^{ab}$ ( $\text{cm}^{-1}$ )	$\epsilon_{\max}^{ab}$ ( $\text{M}^{-1}\text{cm}^{-1}$ )	$k_r^{ba}$ ( $\text{s}^{-1}$ )
Gas-phase	5241 <sup>d</sup>	-	-	$0.0025 \pm 0.0013$ <sup>d,e</sup>
Water- $d_2$ ( $D_2O$ )	$5228 \pm 6$ <sup>a</sup>	$75 \pm 4$ <sup>a</sup>	$6 \pm 2$ <sup>a</sup>	$199 \pm 67$ <sup>a,b</sup>
Methanol	$5217 \pm 4$ <sup>b,c</sup>	$84 \pm 8$ <sup>b,c</sup>	$7 \pm 3$ <sup>b</sup>	$235 \pm 93$ <sup>b</sup>
2-propanol	$5208 \pm 3$ <sup>b</sup>	$62 \pm 5$ <sup>b</sup>	$12 \pm 5$ <sup>b</sup>	$356 \pm 101$ <sup>b</sup>
1-octanol	$5191 \pm 3$ <sup>b</sup>	$60 \pm 5$ <sup>b</sup>	$21 \pm 6$ <sup>b</sup>	$626 \pm 146$ <sup>b</sup>
Acetone	$5218 \pm 3$ <sup>b</sup>	$82 \pm 5$ <sup>b</sup>	$14 \pm 3$ <sup>b</sup>	$507 \pm 120$ <sup>b</sup>
Acetonitrile	$5223 \pm 4$ <sup>b,c</sup>	$81 \pm 8$ <sup>b,c</sup>	$16 \pm 5$ <sup>b</sup>	$528 \pm 153$ <sup>b</sup>
Benzonitrile	$5194 \pm 2$ <sup>b,c</sup>	$80 \pm 4$ <sup>b,c</sup>	$36 \pm 5$ <sup>b</sup>	$1413 \pm 236$ <sup>b</sup>
Acetic acid	$5223 \pm 3$ <sup>b</sup>	$79 \pm 5$ <sup>b</sup>	$10 \pm 4$ <sup>b</sup>	$373 \pm 91$ <sup>b</sup>
Benzene	$5197 \pm 2$ <sup>b,c</sup>	$76 \pm 4$ <sup>b,c</sup>	$32 \pm 3$ <sup>b</sup>	$1289 \pm 187$ <sup>b</sup>
Toluene	$5191 \pm 2$ <sup>b,c</sup>	$73 \pm 4$ <sup>b,c</sup>	$30 \pm 4$ <sup>b</sup>	$1146 \pm 161$ <sup>b</sup>
<i>o</i> -xylene	$5191 \pm 3$ <sup>b</sup>	$73 \pm 5$ <sup>b</sup>	$35 \pm 5$ <sup>b</sup>	$1396 \pm 204$ <sup>b</sup>
<i>p</i> -xylene	$5190 \pm 1$ <sup>c</sup>	$73 \pm 2$ <sup>c</sup>	-	-
Mesitylene	$5194 \pm 3$ <sup>b</sup>	$72 \pm 5$ <sup>b</sup>	$35 \pm 5$ <sup>b</sup>	$1378 \pm 206$ <sup>b</sup>
Bromobenzene	$5184 \pm 3$ <sup>b</sup>	$68 \pm 5$ <sup>b</sup>	$43 \pm 5$ <sup>b</sup>	$1671 \pm 225$ <sup>b</sup>
Tetrahydropyran	$5202 \pm 1$ <sup>c</sup>	$83 \pm 2$ <sup>c</sup>	-	-
Tetrahydrofuran (THF)	$5207 \pm 1$ <sup>c</sup>	$84 \pm 2$ <sup>c</sup>	-	-
1,4-dioxane	$5212 \pm 1$ <sup>c</sup>	$92 \pm 2$ <sup>c</sup>	-	-
Cyclohexane	$5193 \pm 1$ <sup>c</sup>	$73 \pm 2$ <sup>c</sup>	-	-
<i>n</i> -hexane	$5199 \pm 2$ <sup>b,c</sup>	$69 \pm 4$ <sup>b,c</sup>	$23 \pm 4$ <sup>b</sup>	$777 \pm 146$ <sup>b</sup>
Carbon tetrachloride ( $CCl_4$ )	$5195 \pm 2$ <sup>b,c</sup>	$71 \pm 4$ <sup>b,c</sup>	$26 \pm 6$ <sup>b</sup>	$854 \pm 192$ <sup>b</sup>
1,1,2-trichloro-1,2,2-trifluoroethane (Freon 113)	$5209 \pm 2$ <sup>b,c</sup>	$62 \pm 4$ <sup>b,c</sup>	$26 \pm 4$ <sup>b</sup>	$659 \pm 138$ <sup>b</sup>
Carbon disulfide ( $CS_2$ )	$5168 \pm 2$ <sup>b,c</sup>	$89 \pm 4$ <sup>b,c</sup>	$49 \pm 5$ <sup>b</sup>	$2528 \pm 324$ <sup>b</sup>

<sup>a</sup> From Andersen, *et al.*<sup>22</sup><sup>b</sup> From Bregnhøj and Ogilby.<sup>23</sup><sup>c</sup> From Dam, *et al.*<sup>15</sup><sup>d</sup> From Noxon.<sup>24</sup><sup>e</sup> From Schweitzer and Schmidt.<sup>20</sup>

**Table S4:** Spectral data for the  $O_2(b^1\Sigma_g^+) \leftrightarrow O_2(X^3\Sigma_g^-)$  transition.

<b>Solvent</b> <sup>a</sup>	$\nu_{\max}^{Xb}$ ( $\text{cm}^{-1}$ )	$\Delta\nu_{\text{FWHM}}^{Xb}$ ( $\text{cm}^{-1}$ )	$\epsilon_{\max}^{Xb}$ ( $10^{-4} \text{ M}^{-1}\text{cm}^{-1}$ )	$k_r^{bX}$ ( $\text{s}^{-1}$ )
<b>Gas-phase</b>	13120 <sup>b</sup>	-	-	$0.0887 \pm 0.0014$ <sup>b</sup>
<b>Water-<i>d</i><sub>2</sub> (D<sub>2</sub>O)</b>	$13084 \pm 10$	$101 \pm 10$	$13.4 \pm 1.6$	$0.56 \pm 0.10$
<b>Methanol</b>	$13089 \pm 10$	$117 \pm 12$	$7.1 \pm 0.8$	$0.34 \pm 0.05$
<b>1-octanol</b>	$13060 \pm 12$	$119 \pm 12$	$7.3 \pm 1.7$	$0.41 \pm 0.13$
<b>2,2,2-trifluoroethanol</b>	$13113 \pm 14$	$153 \pm 12$	$7.0 \pm 0.8$	$0.41 \pm 0.06$
<b>Acetone</b>	$13096 \pm 10$	$113 \pm 10$	$8.8 \pm 1.0$	$0.43 \pm 0.07$
<b>Acetonitrile</b>	$13094 \pm 12$	$122 \pm 12$	$7.8 \pm 0.9$	$0.40 \pm 0.07$
<b>Benzonitrile</b>	$13057 \pm 10$	$131 \pm 9$	$9.7 \pm 1.5$	$0.69 \pm 0.11$
<b>Toluene</b>	$13045 \pm 7$	$116 \pm 7$	$17.5 \pm 2.0$	$1.05 \pm 0.14$
<b>Chlorobenzene</b>	$13058 \pm 17$	$135 \pm 15$	$15.2 \pm 1.7$	$1.10 \pm 0.17$
<b>Bromobenzene</b>	$13034 \pm 12$	$165 \pm 10$	$40.9 \pm 4.7$	$3.78 \pm 0.50$
<b>Iodobenzene</b>	$13002 \pm 20$	$237 \pm 17$	$387 \pm 48$	$55.2 \pm 7.5$
<b>Cyclohexane</b>	$13062 \pm 9$	$111 \pm 10$	$12.3 \pm 1.4$	$0.65 \pm 0.10$
<b>Carbon tetrachloride (CCl<sub>4</sub>)</b>	$13065 \pm 7$	$114 \pm 9$	$12.6 \pm 1.4$	$0.71 \pm 0.10$
<b>Dichloromethane</b>	$13074 \pm 12$	$128 \pm 9$	$7.6 \pm 1.1$	$0.46 \pm 0.08$
<b>Diiodomethane</b>	$12957 \pm 24$	$284 \pm 20$	$190 \pm 61$	$37.2 \pm 12.2$
<b>Carbon disulfide (CS<sub>2</sub>)</b>	$13011 \pm 12$	$130 \pm 12$	$14.7 \pm 1.7$	$1.16 \pm 0.17$

<sup>a</sup> All solution phase data are from Bregnhøj, *et al.*<sup>6</sup><sup>b</sup> From Ritter and Wilkerson.<sup>25</sup>

## Static dielectric constant

As shown in the main text, solvent dependent changes in oxygen's radiative rate constants correlate reasonably well with the refractive index of the solvent,  $n$ , and functions of  $n$  that quantify the solvent electronic polarizability. In contrast, we find that these rate constants do not correlate with the static dielectric constant of the solvent,  $\epsilon$ , or functions thereof that quantify the "permanent" polarity of the solvent (Figure S3).

On the basis of data from four solvents, a correlation of  $k_r^{bX}$  with the solvent static dielectric constant was claimed by Krasnovsky *et al.*<sup>7</sup> However, this correlation disappears when one considers the current and more extensive set of data on this transition.

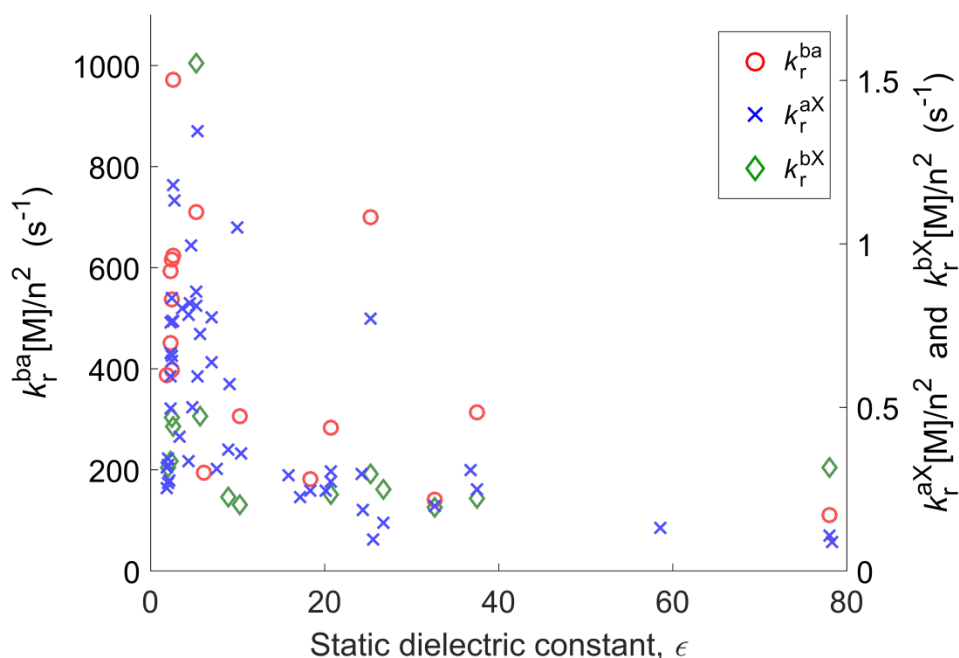


**Fig. S3** Plot of the pseudo first-order radiative rate constants divided by the square of the refractive index,  $k_r[M]/n^2$ , against the solvent static dielectric constant,  $\epsilon$ , for the  $b \rightarrow a$  (red circles, left axis),  $a \rightarrow X$  (blue crosses, right axis), and  $b \rightarrow X$  (green diamonds, right axis) transitions. Data on  $k_r^{bX}$  for the heavy atom solvents iodobenzene and diiodomethane are beyond the chosen scale.

## Spectral bandwidth

In contrast to the transition energy, the spectral bandwidth does not appear to correlate with the refractive index,  $n$  (Figure S4), or any other bulk solvent parameter. However, we observe a distinct heavy-atom effect on the bandwidth of the  $b \rightarrow X$  transition (Figure S4).

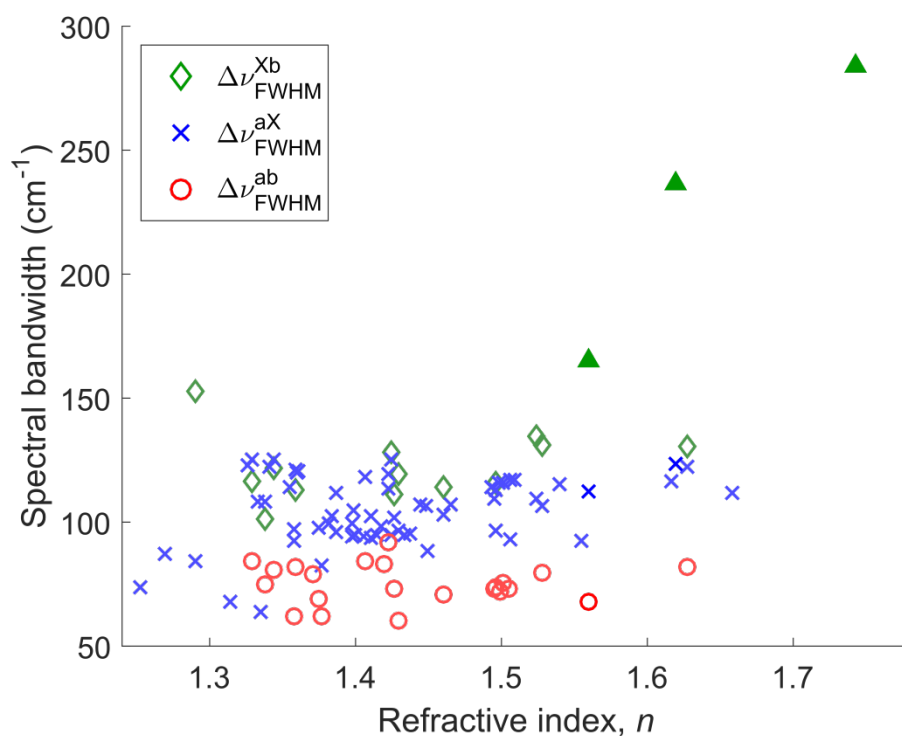


**Fig. S4** Plot of the spectral bandwidth at half maximum,  $\Delta\nu_{FWHM}$ , against the solvent refractive index,  $n$ , for the  $b \rightarrow a$  (red circles),  $a \rightarrow X$  (blue crosses), and  $b \rightarrow X$  (green diamonds) transitions. Data on the  $b \rightarrow X$  transition for the heavy atom solvents bromobenzene, iodobenzene, and diiodomethane are marked with filled green triangles.

## More detailed theoretical considerations on the radiative transitions

To better appreciate how the forbidden radiative transitions in oxygen are perturbed by the solvent, we need to take a closer look at the electronic states and transitions involved.<sup>26-29</sup>

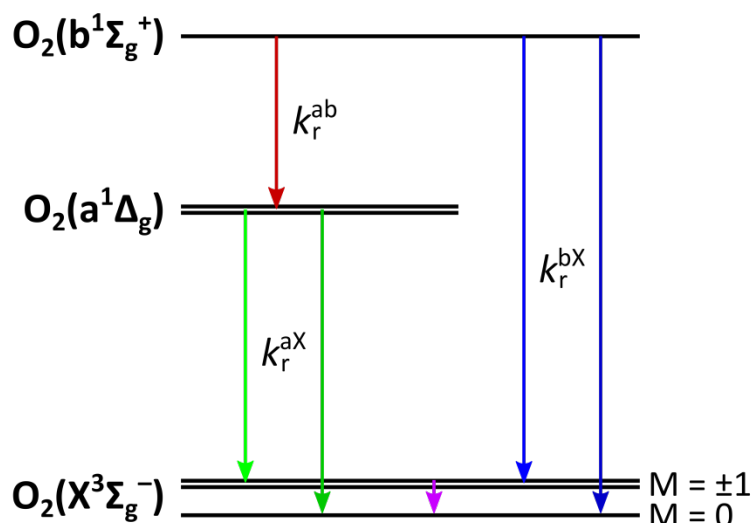


**Fig. S5** Schematic energy diagram depicting the six possible radiative transitions in oxygen.

As shown in Figure S5, the ground state,  $O_2(X^3\Sigma_g^-)$ , is a spin triplet with the  $M_S = \pm 1$  spin-states slightly higher in energy than the  $M_S = 0$  spin-state (the zero-field splitting is  $\approx 4 \text{ cm}^{-1}$ ).<sup>30, 31</sup> The first excited state,  $O_2(a^1\Delta_g)$ , is doubly degenerate on the basis of symmetry, whereas only the second excited state,  $O_2(b^1\Sigma_g^+)$ , is truly a single state.<sup>29</sup> Therefore, there are a total of six possible radiative transitions between these states of oxygen. In solution, the measurable spectroscopic peaks are sufficiently broadened by collisions that transitions to either of the three spin-states of  $O_2(X^3\Sigma_g^-)$  cannot be resolved. Therefore, the experimentally accessible radiative rate constants,  $k_r^{bx}$  and  $k_r^{ax}$ , each reflect contributions from transitions to both  $O_2(X^3\Sigma_g^-)_{(M=\pm 1)}$  and  $O_2(X^3\Sigma_g^-)_{(M=0)}$ . However, each of these “sub-transitions” is unique and responds to changes in the solvent in its own distinct way.

## State mixing and spin-orbit coupling

Much of the spectroscopic behavior of oxygen can be attributed to the inherently strong spin-orbit coupling (SOC) in this open-shell system. SOC mixes the  $O_2(b^1\Sigma_g^+)$  and  $O_2(X^3\Sigma_g^-(M=0))$  states to a larger degree than the other states of oxygen.<sup>27, 28</sup> If we denote the SOC-perturbed wave functions using a wavy term symbol, then we can write the following expressions for the mixed states (eqs S2 and S3).

$$|\tilde{b}^1\Sigma_g^+\rangle = |b^1\Sigma_g^+\rangle + C|X^3\Sigma_{g,M=0}^-\rangle \quad (S2)$$

$$|\tilde{X}^3\Sigma_{g,M=0}^-\rangle = |X^3\Sigma_{g,M=0}^-\rangle - C^*|b^1\Sigma_g^+\rangle \quad (S3)$$

First-order perturbation theory defines the mixing coefficient,  $C$ , through the expression shown in eq S4.

$$C = \frac{\langle X^3\Sigma_{g,M=0}^- | \hat{H}_{SO} | b^1\Sigma_g^+ \rangle}{E_b - E_X} \quad (S4)$$

In eq S4,  $\hat{H}_{SO}$  is the spin-orbit Hamiltonian and  $E_b$  and  $E_X$  are the energies of the  $O_2(b^1\Sigma_g^+)$  and  $O_2(X^3\Sigma_g^-(M=0))$  states, respectively. It is possible to approximate the matrix element in the numerator of eq S4 using the SOC constant for the  $O(^3P)$  atom,  $\zeta_O$ , thus yielding an approximate value of  $C$  (eq S5).<sup>27, 28</sup>

$$C \approx \frac{-i\zeta_O}{E_b - E_X} = 0.0134i \quad (S5)$$

As outlined elsewhere, solvent-dependent charge-transfer (CT) effects likewise play an important role in facilitating the mixing between different electronic states of oxygen.<sup>32, 33</sup> As we shall see, this state mixing plays a crucial role in the way solvents perturb the forbidden transitions in oxygen.<sup>27, 28, 34</sup>

## Overview of oxygen's radiative transitions

### *The $a \rightarrow X_{M=\pm 1}$ and $b \rightarrow X_{M=\pm 1}$ transitions*

The transitions from  $O_2(a^1\Delta_g)$  and  $O_2(b^1\Sigma_g^+)$  to the  $M_S = \pm 1$  spin-states of  $O_2(X^3\Sigma_g^-)$  are allowed as magnetic dipole processes. Due to the pronounced state mixing between  $O_2(b^1\Sigma_g^+)$  and  $O_2(X^3\Sigma_g^-)_{(M=0)}$ , the transition from  $O_2(b^1\Sigma_g^+)$  to  $O_2(X^3\Sigma_g^-)_{(M=\pm 1)}$  can steal intensity from the microwave transition between the  $M_S = \pm 1$  and  $M_S = 0$  spin sub-levels of  $O_2(X^3\Sigma_g^-)$ .  $O_2(a^1\Delta_g)$  does not mix with the ground state, so the  $a \rightarrow X_{(M=\pm 1)}$  transition does not have this possibility. Therefore, the probability of the  $b \rightarrow X_{(M=\pm 1)}$  transition is 2-3 orders of magnitude larger than the  $a \rightarrow X_{(M=\pm 1)}$  transition in the isolated oxygen molecule. An interesting observation in this regard is that  $b \rightarrow X_{(M=\pm 1)}$  emission at 762 nm is one of the strongest features observed in the “glow” of the night sky.<sup>35, 36</sup>

Both the  $b \rightarrow X_{(M=\pm 1)}$  and  $a \rightarrow X_{(M=\pm 1)}$  transitions can steal intensity from allowed transitions to the higher energy  $^1\Pi_g$  and  $^3\Pi_g$ -states, but since the energy differences to these states are very large, this intensity enhancement is only modest and is similar for the two transitions.<sup>37</sup>

Most importantly, since both transitions are purely of magnetic dipole character, they are not very susceptible to collision-induced changes in the electronic structure of oxygen. As such, these transitions are predicted to be mostly unaffected by solvent-dependent perturbations.<sup>27, 28</sup>

### *The $b \rightarrow a$ transition*

The transition between  $O_2(a^1\Delta_g)$  and  $O_2(b^1\Sigma_g^+)$  at 1920 nm is called the Noxon transition and is allowed as an electric quadrupolar transition.<sup>24, 27</sup> This transition is inherently very sensitive to perturbations by colliding molecules, essentially because it is a spin-allowed transition which is forbidden only by the selection rules for symmetry, parity, and angular momentum. Therefore, distortions of the  $\pi$ -orbital symmetry of oxygen can make this transition acquire electric dipole character and, hence, a much larger transition probability. Indeed, enhancements of the  $b \rightarrow a$  transition probability by factors of  $10^5$ - $10^7$  relative to dilute gas-phase have been observed in different environments.<sup>23, 38-40</sup>

### *The $a \rightarrow X_{M=0}$ and $b \rightarrow X_{M=0}$ transitions*

The transitions from  $O_2(a^1\Delta_g)$  and  $O_2(b^1\Sigma_g^+)$  to the  $M_S = 0$  spin-state of  $O_2(X^3\Sigma_g^-)$  are electric quadrupolar in nature, and since they lack an efficient source of intensity borrowing, they are extremely improbable in the isolated oxygen molecule.<sup>27, 31</sup> However, due to the afore-mentioned mixing of  $O_2(b^1\Sigma_g^+)$  and  $O_2(X^3\Sigma_g^-)_{(M=0)}$ , the  $a \rightarrow X_{(M=0)}$  transitions can steal intensity from the  $b \rightarrow a$  transition. Therefore, any collision-enhancement of the  $b \rightarrow a$  transition will be reflected in the probability of the  $a \rightarrow X_{(M=0)}$  transition. Thus, this transition is likewise sensitive to the local environment.

However, the  $b \rightarrow X_{(M=0)}$  transition may acquire electric dipole character through the collision induced difference of the electric dipole moments of the  $O_2(b^1\Sigma_g^+)$  and  $O_2(X^3\Sigma_g^-)_{(M=0)}$  states.<sup>27, 28</sup> Although this mechanism is separate from that enhancing the  $a \rightarrow X_{M=0}$  and  $b \rightarrow a$  transitions, it likewise makes the  $b \rightarrow X_{(M=0)}$  transition very susceptible to perturbations by solvent molecules.

### **Relating theory to experiment**

The theory outlined above has three interesting consequences that are experimentally testable.

#### *1. The ratio of $k_r^{aX}$ and $k_r^{ba}$*

The fact that the  $a \rightarrow X_{(M=0)}$  transition is said to steal intensity from the  $b \rightarrow a$  transition affords a particularly interesting experimental consequence: The ratio of  $k_r^{aX}$  and  $k_r^{ba}$  is predicted to be constant and independent of solvent (eq S6).<sup>27, 28</sup>

$$\frac{k_r^{aX}}{k_r^{ba}} = \frac{g_X g_b}{g_a^2} \frac{v_{aX}^3}{v_{ba}^3} |C|^2 \approx 4.5 \cdot 10^{-4} \quad (\text{S6})$$

In eq S6,  $v$  is the transition energy (in  $\text{cm}^{-1}$ ),  $C$  is the mixing coefficient given by eq S5, and the parameters  $g$  are the degeneracy factors for  $O_2(X^3\Sigma_g^-)$ ,  $O_2(a^1\Delta_g)$ , and  $O_2(b^1\Sigma_g^+)$  (3, 2, and 1, respectively). It is not obvious how many sub-states contribute to the emission, and consequently, what degeneracy factors should be applied in this context. Depending on the choice of degeneracy factors,

values in the range  $(3 - 6) \times 10^{-4}$  can be obtained for this ratio of rate constants.<sup>26-28</sup> Over the past ~30 years, this ratio has been measured in different environments, including high-pressure gas-phase and low-temperature solid matrices.<sup>23, 38-40</sup> In these cases, the ratio was indeed found to be constant and within the right order of magnitude predicted by theory.

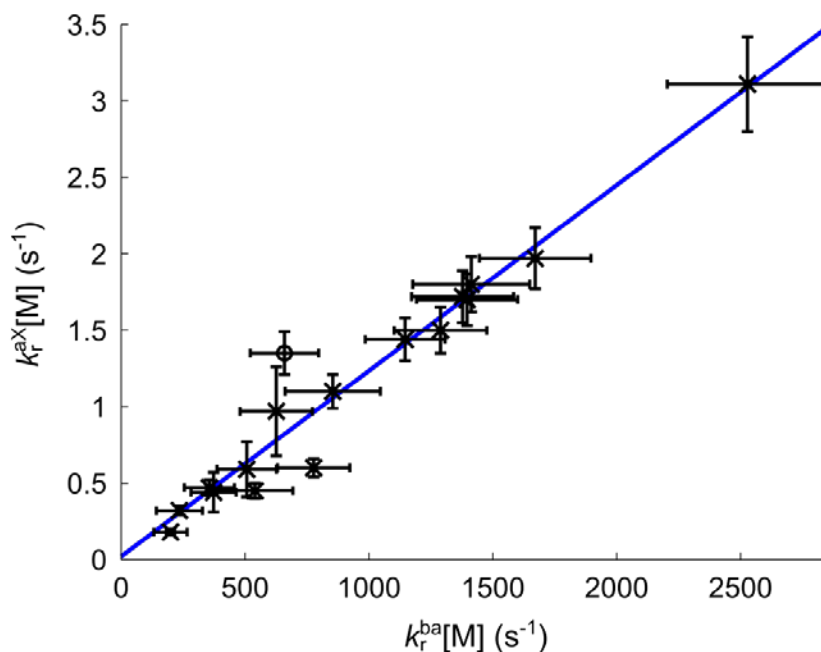


**Fig. S6** A plot of the pseudo first-order rate constants for the  $b \rightarrow a$  and  $a \rightarrow X$  transitions,  $k_r^{aX}[\text{M}]$  and  $k_r^{ba}[\text{M}]$ , against each other. The blue solid line is a linear fit to the data which has a slope of  $(12.2 \pm 0.8) \times 10^{-4}$ . The data from Freon 113 is marked with a circle; a solvent in which the accuracy of the data may be questioned. This figure has been adapted from published material.<sup>23</sup>

A plot of  $k_r^{aX}$  as a function of  $k_r^{ba}$  for 17 liquid solvents is shown in Figure S6. Although the measured value of  $k_r^{aX}/k_r^{ba} = 12.2 \times 10^{-4}$  is somewhat larger than the theoretically predicted value of  $\sim 4.5 \times 10^{-4}$ , these numbers are still remarkably similar. Indeed, the observation that  $k_r^{aX}/k_r^{ba}$  is constant is, by itself, strong validation of the theory.

## 2. Differential response of the radiative transitions to solvation

Upon inspection of the data in Figure 3 of the main text, we note that the  $b \rightarrow X$  transition does not respond to solvent perturbation to the same extent as the  $a \rightarrow X$  and  $b \rightarrow a$  transitions. For example, the

rate constants for the latter two transitions vary by up to a factor of  $\sim 20$  upon changing the solvent from  $D_2O$  to  $CS_2$ . Disregarding the heavy-atom effect (*vide infra*), the rate constant for the  $b \rightarrow X$  transition, in contrast, changes only by a factor of  $\sim 2$ .

The key to understand this phenomenon is to recognize that the  $b \rightarrow X$  transition is 2-3 orders of magnitude more probable than the  $a \rightarrow X$  transition in isolated oxygen (see Table 1 of the main text). Although both transitions contain a solvent-sensitive component (*i.e.*, transitions to  $O_2(X^3\Sigma_g^-)_{(M=0)}$ ), the solvent-insensitive component (*i.e.*, transitions to  $O_2(X^3\Sigma_g^-)_{(M=\pm 1)}$ ) is inherently more probable for the  $b \rightarrow X$  transition in the isolated oxygen molecule. Therefore, even with an appreciable solvent-dependent enhancement of the  $b \rightarrow X_{(M=0)}$  transition, the latter will still not dominate the total  $b \rightarrow X$  transition probability. Calculations<sup>27</sup> specifically predict that the solvent-sensitive  $b \rightarrow X_{(M=0)}$  transition accounts for only  $\approx 10$ -20% of the total  $b \rightarrow X$  transition probability in solution, whereas the solvent-insensitive  $b \rightarrow X_{(M=\pm 1)}$  transition accounts for the remaining 80-90%. Therefore, the total  $b \rightarrow X$  transition probability is rather solvent insensitive.

Conversely, the solvent-insensitive  $a \rightarrow X_{(M=\pm 1)}$  transition is inherently weak, which allows the overall  $a \rightarrow X$  transition probability to be dominated by the solvent-sensitive  $a \rightarrow X_{(M=0)}$  transition. Calculations show that the  $a \rightarrow X_{(M=0)}$  transition accounts for  $> 99.9\%$  percent of the total  $a \rightarrow X$  transition probability in solution.<sup>27</sup>

The overall consequence is that the  $a \rightarrow X$  and  $b \rightarrow a$  transitions are predicted to be very sensitive to perturbations by the solvent, but the  $b \rightarrow X$  transition is not. Again, this prediction is in good agreement with the experimental data.

### 3. Selective heavy-atom effects

Solvents that contain heavy atoms selectively enhance the probability of the  $b \rightarrow X$  transition, but not the two other transitions of oxygen.<sup>6</sup>

This phenomenon can be explained by focusing on the microwave transition between the  $M_S = \pm 1$  and  $M_S = 0$  spin-states of  $O_2(X^3\Sigma_g^-)$ . This is the only transition in oxygen expected to respond directly to external heavy-atoms; it is a transition within the same orbital state configuration

mediated by spin-orbit coupling.<sup>37</sup> This transition strongly depends on the disruption of oxygen's inversion symmetry upon perturbation by the heavy atom.<sup>29, 35-38</sup> Specifically, this transition, allowed as a magnetic dipole process in the isolated molecule, acquires electric dipole character upon perturbation by the solvent (see Table 1 of main text). Only a small electric-dipole component is sufficient to provide an appreciable enhancement of the  $X_{(M=\pm 1)} \rightarrow X_{(M=0)}$  transition. Because the dominant  $b \rightarrow X_{(M=\pm 1)}$  transition steals its intensity from this transition (but the  $a \rightarrow X_{(M=\pm 1)}$  transition does not), only the  $b \rightarrow X$  transition should be affected by external heavy atoms. Calculations<sup>37</sup> predict an enhancement of  $k_r^{bX}$  by a factor of 4-10 for an iodine-containing molecule colliding with oxygen, which is consistent with the experimental data.

## Solvatochromic effects

As indicated in the main text, solvent-dependent spectral shifts of the transitions in oxygen may appear, at first glance, to simply reflect the effects of dispersion interactions. Indeed, this perspective has been taken in an attempt to provide a quantitative interpretation of the  $a \rightarrow X$  data.<sup>41</sup> A key aspect of this dispersion-based interpretation is knowing the polarizabilities of both the  $O_2(a^1\Delta_g)$  and  $O_2(X^3\Sigma_g^-)$  states. Specifically, if one is to account for the bathochromic shift of the  $a \rightarrow X$  transition relative to what is observed in the gas phase, one must assume that  $O_2(a^1\Delta_g)$  is more polarizable than  $O_2(X^3\Sigma_g^-)$ .<sup>41</sup>

It was subsequently shown, however, that for isolated oxygen,  $O_2(X^3\Sigma_g^-)$  is actually more polarizable than  $O_2(a^1\Delta_g)$ .<sup>42</sup> This study also concluded that when the surrounding solvent is considered as a dielectric continuum (*i.e.*, Figure 2a in the main text)  $O_2(X^3\Sigma_g^-)$  is likewise more polarizable than  $O_2(a^1\Delta_g)$ .

This issue of oxygen's polarizability was just one factor that pointed to the need for a more sophisticated model to interpret the effect of solvent on oxygen's spectral shifts. A reasonable solution to this problem was achieved by considering a discrete M-O<sub>2</sub> complex that, in turn, was subject to both the fast and slow dielectric effects of the surrounding medium (*i.e.*, Figure 2b in the main text).<sup>43</sup> Interestingly, it was later shown that, when in the M-O<sub>2</sub> complex,  $O_2(a^1\Delta_g)$  is indeed

more polarizable than  $O_2(X^3\Sigma_g^-)$ .<sup>28</sup> The key result in all of this, however, is that one must invoke the direct perturbation of oxygen in a collision complex with a molecule M.

As outlined in the main text, the formation of an M-O<sub>2</sub> complex also makes it possible to invoke mixing with the M-O<sub>2</sub> charge-transfer (CT) state. Among other things, the introduction of CT character alters the polarizability of the M-O<sub>2</sub> complex and this, in turn, influences the interaction of the complex with the surrounding dielectric medium.<sup>28</sup> Because  $O_2(b^1\Sigma_g^+)$  is closest in energy to the CT state, these effects are reflected in the fact that the solvent dependent spectral shifts are largest for the  $b \rightarrow X$  transition (see discussion in main text).

## References

- (1) Nonell, S.; Flors, C. *Singlet Oxygen: Applications in Biosciences and Nanosciences*; Royal Society of Chemistry, 2016.
- (2) Ogilby, P. R. Singlet oxygen: there is indeed something new under the sun. *Chem. Soc. Rev.* **2010**, *39*, 3181-3209.
- (3) Bregnhøj, M.; Westberg, M.; Jensen, F.; Ogilby, P. R. Solvent-dependent singlet oxygen lifetimes: temperature effects implicate tunneling and charge-transfer interactions. *Phys. Chem. Chem. Phys.* **2016**, *18*, 22946-22961.
- (4) Blázquez-Castro, A. Direct <sup>1</sup>O<sub>2</sub> optical excitation: a tool for redox biology. *Redox Biol.* **2017**, *13*, 39-59.

(5) Bregnhøj, M.; Blazquez-Castro, A.; Westberg, M.; Breitenbach, T.; Ogilby, P. R. Direct 765 nm optical excitation of molecular oxygen in solution and in single mammalian cells. *J. Phys. Chem. B* **2015**, *119*, 5422-5429.

(6) Bregnhøj, M.; Krægpøth, M. V.; Sørensen, R. J.; Westberg, M.; Ogilby, P. R. Solvent and Heavy-Atom Effects on the  $O_2(X^3\Sigma_g^-) \rightarrow O_2(b^1\Sigma_g^+)$  Absorption Transition. *J. Phys. Chem. A* **2016**, *120*, 8285-8296.

(7) Krasnovsky, A. A.; Kozlov, A. S. Photonics of dissolved oxygen molecules. Comparison of the rates of direct and photosensitized excitation of oxygen and reevaluation of the oxygen absorption coefficients. *J. Photochem. Photobiol. A* **2016**, *329*, 167-174.

(8) Wilkinson, F.; Helman, W. P.; Ross, A. B. Rate constants for the decay and reactions of the lowest electronically excited singlet state of molecular oxygen in solution. An expanded and revised compilation. *J. Phys. Chem. Ref. Data* **1995**, *24*, 663-677.

(9) Schmidt, R. Influence of heavy atoms on the deactivation of singlet oxygen ( $^1\Delta_g$ ) in solution. *J. Am. Chem. Soc.* **1989**, *111*, 6983-6987.

(10) Schmidt, R.; Afshari, E. Collisional deactivation of  $O_2(^1\Delta_g)$  by solvent molecules. Comparative experiments with  $^{16}O_2$  and  $^{18}O_2$ . *Ber. Bunsen. Phys. Chem* **1992**, *96*, 788-794.

(11) Schmidt, R.; Brauer, H. Radiationless deactivation of singlet oxygen ( $^1\Delta_g$ ) by solvent molecules. *J. Am. Chem. Soc.* **1987**, *109*, 6976-6981.

(12) Weldon, D.; Poulsen, T. D.; Mikkelsen, K. V.; Ogilby, P. R. Singlet sigma: the “other” singlet oxygen in solution. *Photochem. Photobiol.* **1999**, *70*, 369-379.

(13) Wessels, J. M.; Rodgers, M. A. Effect of solvent polarizability on the forbidden  $^1\Delta_g \rightarrow ^3\Sigma_g^-$  transition in molecular oxygen: a fourier transform near-infrared luminescence study. *J. Phys. Chem.* **1995**, *99*, 17586-17592.

(14) Truscott, T. G.; MacPherson, A. N.; Turner, P. H. Fourier-transform Luminescence Spectroscopy of Solvated Singlet Oxygen. *J. Chem. Soc. Faraday Trans.* **1994**, *90*, 1065-1072.

(15) Dam, N.; Keszthelyi, T.; Andersen, L. K.; Mikkelsen, K. V.; Ogilby, P. R. Effect of Solvent on the  $O_2(a^1\Delta_g) \rightarrow O_2(b^1\Sigma_g^+)$  Absorption Spectrum: Demonstrating the Importance of Equilibrium vs Nonequilibrium Solvation. *J. Phys. Chem. A* **2002**, *106*, 5263-5270.

(16) Ogilby, P. R. Solvent effects on the radiative transitions of singlet oxygen. *Acc. Chem. Res.* **1999**, *32*, 512-519.

(17) Poulsen, T. D.; Ogilby, P. R.; Mikkelsen, K. V. Solvent Effects on the  $O_2(a^1\Delta_g) - O_2(X^3\Sigma_g^-)$  Radiative Transition: Comments Regarding Charge-Transfer Interactions. *J. Phys. Chem. A* **1998**, *102*, 9829-9832.

(18) Hild, M.; Schmidt, R. The Mechanism of the Collision-Induced Enhancement of the  $a^1\Delta_g \rightarrow X^3\Sigma_g^-$  and  $b^1\Sigma_g^+ \rightarrow a^1\Delta_g$  Radiative Transitions of  $O_2$ . *J. Phys. Chem. A* **1999**, *103*, 6091-6096.

(19) Darmanyan, A. P. Effect of Charge-Transfer Interactions on the Radiative Rate Constant of  $^1\Delta_g$  Singlet Oxygen. *J. Phys. Chem. A* **1998**, *102*, 9833-9837.

(20) Schweitzer, C.; Schmidt, R. Physical mechanisms of generation and deactivation of singlet oxygen. *Chem. Rev.* **2003**, *103*, 1685-1758.

(21) Schmidt, R. Determination of the phosphorescence quantum yield of singlet molecular oxygen ( $^1\Delta_g$ ) by means of a radiometer and an infrared luminescence spectrometer. *Chem. Phys. Lett.* **1988**, *151*, 369-374.

(22) Andersen, L. K.; Ogilby, P. R. Absorption Spectrum of Singlet Oxygen ( $a^1\Delta_g \rightarrow b^1\Sigma_g^+$ ) in  $D_2O$ : Enabling the Test of a Model for the Effect of Solvent on Oxygen's Radiative Transitions. *J. Phys. Chem. A* **2002**, *106*, 11064-11069.

(23) Bregnhøj, M.; Ogilby, P. R. Effect of Solvent on the  $O_2(a^1\Delta_g) \rightarrow O_2(b^1\Sigma_g^+)$  Absorption Coefficient. *J. Phys. Chem. A* **2015**, *119*, 9236-9243.

(24) Noxon, J. Observation of the transition in  $O_2$ . *Can. J. Phys.* **1961**, *39*, 1110-1119.

(25) Ritter, K.; Wilkerson, T. High-resolution spectroscopy of the oxygen A band. *J. Mol. Spectrosc.* **1987**, *121*, 1-19.

(26) Minaev, B. F.; Lunell, S.; Kobzev, G. The influence of intermolecular interaction on the forbidden near-IR transitions in molecular oxygen. *J. Mol. Struct. Theochem* **1993**, *284*, 1-9.

(27) Minaev, B. F.; Ågren, H. Collision-induced  $b^1\Sigma_g^+ - a^1\Delta_g$ ,  $b^1\Sigma_g^+ - X^3\Sigma_g^-$  and  $a^1\Delta_g - X^3\Sigma_g^-$  transition probabilities in molecular oxygen. *J. Chem. Soc. Faraday Trans.* **1997**, *93*, 2231-2239.

- (28) Minaev, B. F. Electronic mechanisms of activation of molecular oxygen. *Russ. Chem. Rev.* **2007**, *76*, 988-1010.
- (29) Paterson, M. J.; Christiansen, O.; Jensen, F.; Ogilby, P. R. Overview of Theoretical and Computational Methods Applied to the Oxygen-Organic Molecule Photosystem. *Photochem. Photobiol.* **2006**, *82*, 1136-1160.
- (30) Tinkham, M.; Strandberg, M. W. P. Theory of the fine structure of the molecular oxygen ground state. *Phys. Rev.* **1955**, *97*, 937.
- (31) Klotz, R.; Marian, C. M.; Peyerimhoff, S. D.; Hess, B. A.; Buenker, R. J. Calculation of spin-forbidden radiative transitions using correlated wavefunctions: Lifetimes of  $b^1\Sigma_g^+$ ,  $a^1\Delta_g$  states in  $O_2$ ,  $S_2$  and  $SO$ . *Chem. Phys.* **1984**, *89*, 223-236.
- (32) Jensen, P.; Arnbjerg, J.; Tolbod, L. P.; Toftegaard, R.; Ogilby, P. R. Influence of an Intermolecular Charge-Transfer State on Excited-State Relaxation Dynamics: Solvent Effect on the Methylanthalene–Oxygen System and its Significance for Singlet Oxygen Production. *J. Phys. Chem. A* **2009**, *113*, 9965-9973.
- (33) Minaev, B. F. Spin-orbit coupling mechanism of singlet oxygen  $a^1\Delta_g$  quenching by solvent vibrations. *Chem. Phys.* **2017**, *483-484*, 84-95.
- (34) Minaev, B. F.; Murugan, N. A.; Ågren, H. Dioxygen spectra and bioactivation. *Int. J. Quant. Chem.* **2013**, *113*, 1847-1867.

- (35) Cosby, P. C.; Sharpee, B. D.; Slanger, T. G.; Huestis, D. L.; Hanuschik, R. W. High-resolution terrestrial nightglow emission line atlas from UVES/VLT: Positions, intensities, and identifications for 2808 lines at 314–1043 nm. *J. Geophys. Res.* **2006**, *111*.
- (36) Slanger, T. G.; Copeland, R. A. Energetic oxygen in the upper atmosphere and the laboratory. *Chem. Rev.* **2003**, *103*, 4731-4766.
- (37) Minaev, B. F. Intensities of spin-forbidden transitions in molecular oxygen and selective heavy-atom effects. *Int. J. Quant. Chem.* **1980**, *17*, 367-374.
- (38) Becker, A.; Schurath, U.; Dubost, H.; Galaup, J. Luminescence of metastable  $^{16}\text{O}_2(^1\text{O}_2)$  in solid argon: Relaxation and energy transfer. *Chem. Phys.* **1988**, *125*, 321-336.
- (39) Fink, E.; Setzer, K.; Wildt, J.; Ramsay, D.; Vervloet, M. Collision-induced emission of  $\text{O}_2$  ( $\text{b}^1\Sigma_g^+ \rightarrow \text{a}^1\Delta_g$ ) in the gas phase. *Int. J. Quant. Chem.* **1991**, *39*, 287-298.
- (40) Schmidt, R.; Bodesheim, M. Collision-Induced Radiative Transitions  $\text{b}^1\Sigma_g^+ \rightarrow \text{a}^1\Delta_g$ ,  $\text{b}^1\Sigma_g^+ \rightarrow \text{X}^3\Sigma_g^-$ , and  $\text{a}^1\Delta_g \rightarrow \text{X}^3\Sigma_g^-$  of  $\text{O}_2$ . *J. Phys. Chem.* **1995**, *99*, 15919-15924.
- (41) Schmidt, R. Solvent Shift of the  $^1\Delta_g \rightarrow ^3\Sigma_g^-$  Phosphorescence of  $\text{O}_2$ . *J. Phys. Chem.* **1996**, *100*, 8049-8052.
- (42) Poulsen, T. D.; Ogilby, P. R.; Mikkelsen, K. V. Polarizabilities of the First Excited ( $\text{a}^1\Delta_g$ ) and Ground ( $\text{X}^3\Sigma_g^-$ ) States of Molecular Oxygen. *J. Phys. Chem. A* **1998**, *102*, 8970-8973.

(43) Poulsen, T. D.; Ogilby, P. R.; Mikkelsen, K. V. The  $a^1\Delta_g \rightarrow X^3\Sigma_g^-$  Transition in Molecular Oxygen: Interpretation of Solvent Effects on Spectral Shifts. *J. Phys. Chem. A* **1999**, *103*, 3418-3422.